Published in final edited form as:
J Am Coll Cardiol. 2011 March 1; 57(9): 1081–1092. doi:10.1016/j.jacc.2010.09.066.

Mechanisms of Fractionated Electrograms Formation in the Posterior Left Atrium during Paroxysmal Atrial Fibrillation in Humans

Felipe Atienza, MD, PhD[1,*], **David Calvo, MD**[1,*], **Jesús Almendral, MD, PhD**[1], **Sharon Zlochiver, PhD**[2], **Krzysztof R. Grzeda, MD**[2], **Nieves Martinez-Alzamora, PhD**[3], **Esteban G. Torrecilla, MD, PhD**[1], **Angel Arenal, MD**[1], **Francisco Fernández-Avilés, MD, PhD**[1], and **Omer Berenfeld, PhD**[2]

[(1)]Hospital General Universitario Gregorio Marañón, Madrid, Spain

[(2)]Center for Arrhythmia Research, University of Michigan, Ann Arbor, Michigan, USA

[(3)]Department of Statistics, Polytechnic University, Valencia, Spain

Abstract

Objective—To study mechanisms of formation of fractionated electrograms on the posterior left atrial wall (PLAW) in human paroxysmal atrial fibrillation (AF).

Background—The mechanisms responsible for complex fractionated atrial electrograms formation during AF are poorly understood.

Methods—In 24 pts we induced sustained AF by pacing from a pulmonary vein (PV). We analyzed transitions between organized patterns and changes in electrogram morphology leading to fractionation in relation to interbeat interval duration (systolic interval) and dominant frequency (DF). Computer simulations of rotors helped in the interpretation of the results.

Results—Organized patterns were recorded 31±18% of the time. In 47% of organized patterns, the electrograms and PLAW activation sequence were similar to those of incoming waves during PV stimulation that induced AF. Transitions to fractionation were preceded by significant increases in electrogram duration, spikes number, and systolic interval shortening (R^2=0.94). Similarly, adenosine infusion during organized patterns caused significant systolic interval shortening leading to fractionated electrogram formation. Activation maps during organization showed incoming wave patterns, with earliest activation located closest to the highest DF site. Activation maps during transitions to fragmentation showed areas of slowed conduction and unidirectional block. Simulations predicted that systolic interval abbreviation that heralds fractionated electrograms formation may result from a Doppler effect on wavefronts preceding an approaching rotor, or by acceleration of a stationary or meandering, remotely located source.

Address for correspondence: Felipe Atienza, MD, PhD, Cardiology Department, Hospital General Universitario Gregorio Marañón, C/ Dr Esquerdo, 46, 28007 Madrid, Spain. +34915867020 (fax) +34915868276 (fax) fatienzaf@secardiologia.es. Omer Berenfeld, PhD, Center for Arrhythmia Research, 5025 Venture Drive, Ann Arbor, Michigan 48108. oberen@med.umich.edu.
[*]Drs. Atienza and Calvo contributed equally to this article.

Conclusions—During induced AF, systolic interval shortening following either drift or acceleration of a source results in intermittent fibrillatory conduction and formation of fractionated electrograms at the PLAW.

Keywords

atrial fibrillation; fractionated electrograms; adenosine; conduction delay; reentry

INTRODUCTION

Paroxysmal atrial fibrillation (AF) is maintained by high-frequency sources most commonly located at pulmonary vein-left atrial junctions (PV-LAJ) (1,2). Thus catheter based PV isolation has proved to cure AF in a significant proportion of AF patients (3). Recent studies have proposed targeting complex fractionated atrial electrograms (CFAE) at a range of atrial sites as a means to increase AF ablation success, but results are controversial (4,5). While some fractionated signals might represent critical zones related to AF maintenance (i.e. high-frequency sources "driving" AF), others may be passive and unrelated to the primary arrhythmia mechanism (i.e. wavefront collision or overlapping) (6–8). In fact, the pathophysiologic relationship between high-frequency PV discharges and CFAEs on the posterior left atrial wall (PLAW) is far from being understood. Previous studies suggested that there may be a relationship between fractionated electrograms and short AF cycle lengths, but AF initiation and transitions to fractionation were not analyzed and no mechanistic explanations were proposed (6,9–11). On the other hand, recent studies suggest that signal fractionation results from the dynamic interplay between high-frequency sources and the specific anatomic arrangements of the PV-LAJ (12–14). Since the PLAW plays a critical role in the initiation and maintenance of paroxysmal AF, we aimed to study the mechanisms of fractionation formation at the PLAW, following AF induction. We hypothesized that: 1) the fractionation of electrograms on the PLAW during AF is rate-dependent and secondary to fibrillatory conduction of waves emerging from high-frequency sources, and 2) adenosine infusion during organized phases triggers fractionation by accelerating the reentrant sources that activate PLAW.

METHODS

Patients admitted for ablation of drug-refractory paroxysmal AF were included in this protocol, as approved by the Institutional Ethics Committee. All patients gave informed consent. Exclusion criteria were arriving in AF to the electrophysiology laboratory and induction of non-sustained AF (<5 minutes duration). All antiarrhythmic agents were withheld >5 half-lives before the study.

Electrophysiologic Study and Recording Protocol

The electrophysiologic study used catheters positioned at high right atrium (HRA), distal coronary sinus (CS), and ablation catheter at the PVs. The PLAW was mapped using a 20 pole-spiral catheter and analyzed off-line. The 3-dimensional geometry of the LA was reconstructed using an electroanatomic navigation system (see Online Supplement).

We infused central venous boluses of 12 mg adenosine during AF, while catheters remained at fixed predefined positions (15).

Spatiotemporal Analysis of PLAW Recordings during PV Stimulation and during AF

During AF, we defined "*organized pattern*" as a repetitive, uniform and constant sequence of ≥4 consecutive electrograms with isoelectric line between them and identical sequence of

activation (Figure 1A) on the 10 bipoles of the PLAW catheter. "*Fractionated electrograms*" were defined as electrograms exhibiting multiple (≥2) deviations from baseline and/or continuous electrical activity without isoelectric line and duration greater than 50 ms (4,9,10). The time course of organization during the first 5 minutes following AF induction was calculated as the duration of the sum of organized phases in seconds, divided by total recording period duration (300 seconds).

We analyzed the following patterns of activation: 1) *Incoming wave patterns*: double-bracket sequences, with earliest activation consistently occurring in adjacent bipoles at the outer and inner loops of the spiral catheter; 2) *incomplete conduction block* along a line of functional block: wavefront breaks occurring across the line at a point of slowed conduction; and, 3) *re-entrant pattern* around a line of functional block: rotating wave not associated with an anatomic obstacle, with significant isochrone crowding and double potentials, not present during sinus rhythm (10). Activation patterns on the PLAW during PV stimulation prior to AF induction were compared to organized patterns that occurred during the first 5 minutes after AF induction in all patients. In a subset of patients (n=5), off-line PLAW activation and propagation maps during transitions from organized to fragmented electrograms were constructed using the NavX system (see Online Supplement).

Analysis of Regional Rate of Activation

For interbeat interval analysis, the timing from the maximal rapid deflection of a bipolar electrogram to the next was considered to be the *systolic interval (SI)*. During organized-to-fragmented electrogram transitions, we analyzed ten consecutive electrograms prior to fragmentation and 5 consecutive organized beats immediately post-fragmentation, as shown in Figure 1B. Intervals during fragmented phases were measured at the closest adjacent channel not showing fragmentation.

For stationary spectral analysis, dominant frequency (DF) was determined as previously described (Online Supplement) (7,8,12,13,15). Time courses of DF during the 5-minute recording period were calculated from 5–sec samples obtained at half of each 1-minute interval following AF induction and averaged for all recordings at the PLAW. In a subset of patients (n=10), real-time DF determination on the LA was obtained using NavX with embedded spectral analysis capabilities.

Computer simulations

We used a 5×5-cm model of realistic human atrial kinetics with heterogeneous $I_{K,ACh}$ density in the presence of 0.1 μm acetylcholine (See Online Supplement) (16).

Statistical Analysis

Continuous variables are reported as mean±SD or median and interquartile range (IQR), depending on data distribution. For details, including internal validation measurements, see Online Supplement. Statistical significance was established at $P<0.05$.

RESULTS

Patients

AF was induced using PV stimulation in 24 paroxysmal AF patients (53±10 years; 73% male) arriving to the electrophysiology laboratory in sinus rhythm. Unless otherwise stated, all results correspond to the entire sample of 24 patients.

Time Courses of Organization and DF Change

During the first 5 minutes after AF induction, both organized and fragmented electrograms were intermittently recorded at the PLAW (Figure 1A). organized patterns were recorded 31±18% of the time. In Figure 2, the duration of organized phases decreased gradually from AF onset to the fifth minute of recording (black bars; $p=0.007$), whereas PLAW DF's significantly increased (white bars; $p<0.001$). There was a highly significant inverse correlation between the duration of organized phases and PLAW DF (Pearson correlation= −0.373; $p<0.001$).

Transitions between Organized and Fragmented Electrograms

Transitions from organized to fragmented phases were analyzed in episodes showing 10 consecutive intervals whereby the first 7 were not fragmented and the last 3 showed progressively more fragmentation (see Figure 1B). Overall, electrograms undergoing transition showed progressive disorganization, until no regular activation could be identified. As illustrated in panels A–C of Figure 3, in channels showing fragmentation, the mean electrogram duration (A) and the number of spikes (B) increased gradually as the systolic interval (C) decreased and the pattern changed from organized to fragmented. As summarized in panel D, a bimodal behaviour was observed for the SI as the pattern changed from organized to fragmented and back to organized. The average SI pre-fragmentation was significantly longer than during fragmentation (198.9±34.2 vs. 177.6±25.6 ms; $p=0.006$). Similarly, the SI for 5 consecutive organized beats post-fragmentation also was significantly longer (193±39.1 ms; $p=0.038$) than during fragmentation. No significant difference in SI was observed between organized pre-fragmentation and post-fragmentation phases on either side of the fragmented phase.

Adenosine Infusion Increases DF and Leads to Fragmentation

Boluses of adenosine were infused in 9 patients. At peak adenosine effect, mean DF increased significantly at the PLAW compared to baseline (7.64±1.57 vs. 6.22±1.39 Hz; $p<0.05$). In 4 patients, adenosine was infused during a stable organized phase. At peak adenosine effect there was a transition from organized to fragmented electrograms coincident with SI shortening (Figure 4A). In fact, as shown in panels B–D, there was a significant SI shortening, with increase in electrogram duration and number of spikes in all cases. As expected, a bimodal behavior was also observed in the SI when comparing the pre-fragmentation, fragmentation and post-fragmentation phases occurring, respectively, before, during and after the peak adenosine effect (Figure 4E).

Spatial Patterns of Activation and Transitions to Fragmentation

Overall, organized phases during AF were characterized by incoming wave patterns of activation recorded by the spiral catheter at the PLAW (Figure 5A). The following incoming activation patterns were recorded: 1) *concordant*: incoming AF pattern identical to that generated by high-frequency stimulation from any PV; 2) *ipsilateral*: incoming AF pattern showing an activation sequence similar to that during pacing from either the superior or the inferior PV; and, 3) *discordant*: activation pattern dissimilar to those during pacing from any PV (see Online Supplement). As illustrated in Figure 5 (panels B and D), the incoming wave pattern of activation at the PLAW during organized AF mimicked that obtained during PV stimulation from which AF was induced; i.e., the pattern was concordant 46±27% of the organized time. Moreover, as seen in panels C and E, the incoming wave pattern mimicked that obtained during pacing from *any* of the ipsilateral PVs that induced AF 63±24% of the organized time ($p=0.025$).

In 10 patients, real-time LA DF maps revealed the presence of high DF sites close to the PV-LA junctions (Figure 6A). In 7 such patients the location of the DFmax site was the same as the earliest site of activation, which was concordant with the directionality of the predominant incoming wavefront as recorded by the spiral catheter at the PLAW (Figure 6B). In this group the number of DFmax sites and the number of organized patterns per patient were similar (2.1±0.99 vs. 2.2±0.78; p=0.48).

In 5 cases we analyzed the patterns of activation at the PLAW for each beat during organized-to-fragmented electrogram transitions. The direction and propagation pattern of the incoming wave were similar for each of the 7 pre-fragmentation beats with earliest activation occurring at bipoles closest to the PV-LAJ (Figure 6B, movie 1). However, several beat-to-beat changes were observed in the transition toward the fragmented phase. First, as the rate of the penetrating wave increased (i.e., SI shortened), the electrograms widened and double electrograms began to appear during the last 3 beats of the transition to fragmentation. The propagation pattern of the incoming wave changed, yielding one of two new outcomes: a) reentry pattern around a line of functional block, as in Figure 7A, in which the reentrant excitation wave front circulated clockwise around a pivoting point located anatomically at the septo-pulmonary bundle (movie 2); b) activation breakthrough across a line of slow conduction (Figure 7B, movie 3). Overall, these patterns appeared in 62% of the cases, of which 71% were re-entrant and 29% were breaktrough-like. Once fragmentation in all the PLAW electrograms ensued interpretation became unreliable.

Numerical Simulations and Possible Mechanisms

Figure 8A shows snapshots of activity in the model at different times along with bipolar electrograms from a spiral catheter simulating the one used in the patients. When broad waves from a distantly located main rotor approached the recording site, well organized electrograms were inscribed at relatively long SIs. However, as the rotor drifted toward the catheter, the SI shortened monotonically (see bipoles 3–4 and 13–14, see also Online Supplement) and the electrograms widened. At about 0.8 sec after onset, sudden SI prolongation ensued (vertical red line), revealing conduction impairment and wavebreak at the catheter area. This was followed by the creation of two short-lived rotors (middle top panel), one of which lingered briefly on the upper right corner, pivoting between bipoles 3–4 and 13–14 (red dot). Consequently the electrograms became wider, the number of spikes per electrogram increased, and fragmentation ensued, primarily at bipoles 3–4 and 13–14. Thereafter, as the secondary rotors disappeared at 1.5 sec, relative organization resumed and the SI increased (red arrows) to values similar to those seen prior to fragmentation.

Figure 8B–C demonstrates how a drifting rotor may produce beta-to-beat SI shortening and fragmentation. In B, we have superimposed the complete trajectory of the drifting rotor's tip on a snapshot of the transmembrane voltage at time 0. As the rotor drifted from its original location (red dot) its distance to the recording electrogram 13–14 (blue dot) shortened. As expected, the rotor's translational movement was accompanied by a Doppler shift, whereby the wavefronts ahead of the tip accommodated with a briefer periodicity than the wavefronts behind the tip (see Online Supplement) (17). In C, we have plotted the SI at the electrogram location as a function of the distance between the tip and the recording site. As the drifting rotor approximated the bipoles, SI abbreviated, resulting in wavebreak (panel A).

DISCUSSION

The major findings of the study are as follows: First, in induced, paroxysmal AF, electrogram fractionation at the PLAW is rate-dependent. Second, organized AF phases show a highly stable and recurrent pattern of incoming waves of activation emanating from high-frequency sites at the PV-LAJ area. Third, transitions from organized to fractionated

electrograms are preceded by progressive cycle length shortening leading to beat-to-beat changes in wavefront directionality, intermittent wavebreak and reentry around a line of functional block, most likely at the septo-pulmonary bundle. Finally, the results of adenosine infusions and of computer simulations reproduced the spontaneous organized-to-fractionated-to-organized transitions, and strongly supported the idea that wavefront acceleration ahead of drifting rotors on the PLAW and/or rotor meandering gives rise to intermittent local fractionation. The overall results suggest that in paroxysmal AF, electrogram fractionation at the PLAW is a reflection of fibrillatory conduction and a consequence of the dynamic interaction between high frequency re-entrant sources and the atrial anatomy.

High Level of Organization of the PLAW during AF

Despite the spatiotemporal complexity of wave propagation during AF, studies have demonstrated that AF is deterministic (7,8,11–13,17). Using epicardial recordings, Wells *et al*. found that the fibrillatory signal often increased or decreased its organization at different times (11). Similarly, here we have demonstrated that in human AF, organized and disorganized phases alternate, with the PLAW harboring regular, fast, and spatiotemporally organized activity during a significant proportion of time. As shown by our results, periodic impulses originating at the PV-LAJ propagate in highly recurrent directions repetitively toward the center of the PLAW. The high correlation between the location of DF areas and the origin of incoming waves strongly suggests that during organized AF phases PLAW is passively activated from high-frequency sources located at the PV-LAJ.

Activation Frequency and Fractionated Electrograms

The original definition of CFAEs includes 2 different features: electrogram fractionation and short electrogram cycle length (4). We considered both but analyzed them as separate variables to get mechanistic insight of their possible interaction. We found that the local frequency of activation is the main determinant of electrogram fragmentation at the PLAW, since the instantaneous atrial activation frequency (i.e., 1/cycle length) invariably increased prior to fragmentation and decreased upon organization. In other words, contrary to what is implied in Nademanee's definition (4), CFAEs and short electrogram cycle length are not independent of each other.

The relationship between activation rate and electrogram complexity has been previously documented, however its pathophysiology remains unclear (6,11). Rostock *et al.* found that the occurrence of fractionated electrograms anywhere in the atria was significantly associated with AF cycle length shortening (9). However, AF initiation and transitions to fractionation were not analyzed. Studies demonstrated that the atria respond to activation rate increments with progressive deterioration of stable directionality and electrogram fractionation (7,18). Moreover, high-density mapping has identified clusters of high DF sites with fractionation most likely observed adjacent to those sites (13,19). Thus, the transition to fractionation is not random, and reflects functional deterioration in the atrial conduction properties in response to periodic input acceleration. Several of our findings support this idea. First, the lower degree of organization during the last 3 interbeat intervals prior to fragmentation was paralleled by an increase in AF activation rate (20). Second, adenosine infusion during the organized phase, accelerated the DFmax of the AF sources at the PV-LAJ and resulted in fragmentation (15). Finally, computer simulations showed that rotor drift towards the recording area yielded in a similar increase (~20%) in the local frequency of activation at the PLAW (17).

Role of the Atrial Anatomy in Fractionation

In paroxysmal AF patients, Markides *et al.* demonstrated the presence of a line of functional conduction block at the anatomical location of the septo-pulmonary bundle in the PLAW (21). At this site, conduction is markedly slowed when wave fronts propagate perpendicular to the septo-pulmonary bundle (12,14,21). Thus, this functional line of block creates the substrate for functional reentry causing wave fronts exiting the PV ostium to break.

We observed a change in the activation pattern as rate increased during transitions from organized to fragmented patterns. Electrograms progressively widen and double electrograms emerged, reflecting the formation of functional lines of block (10,14). In some cases, functional reentry occurred around the line of functional block (movie 2). A breakthrough pattern across a line of slow conduction could also be observed in other cases at the same location (movie 3). In accordance to previous experimental work most of the wavebreaks appeared at either edge of the septo-pulmonary bundle (12).

Of importance in our study was the transient nature of the fractionated signals at the PLAW. While electrograms were narrow and discrete during organized AF phases, highly fractionated electrograms were recorded at the same location following local frequency acceleration (7). This observation is consistent with the finding that PV isolation reduces fractionated electrograms density by globally increasing AF organization (22). Our overall results suggest that a possible mechanism for transient electrogram fractionation is passive wavebreak around areas of functional block and unstable reentrant circuit formation.

Clinical Implications

The idea of targeting fractionated electrograms, either alone or in combination to other ablation strategies, remains controversial (4,5). Experimental and clinical studies have shown that fractionated signals might potentially represent zones critical to AF maintenance. Kalifa *et al.* found that the periphery of high-frequency AF drivers is the area at which most fractionation occurs (13). Rotor meandering might also underlie, at least in part, the electrogram fractionation at close proximity of the source (8). This may explain the success of some CFAE ablation procedures that produce an anatomic obstacle around the highest DF site (4,13). However, other studies suggest that CFAEs may be unrelated to the primary arrhythmia mechanism, and simply represent transient pivoting, wavefront collision or sink-to-source mismatch (6,7,10). Most importantly, fractionation is significantly reduced following PV isolation, with prolongation of AF cycle length underscoring its passive role (22). For all these reasons, CFAE ablation strategies have had a low impact on AF recurrence prevention in paroxysmal AF ablation and should not be recommended as a stand alone strategy (5).

Limitations

Higher density in a wider mapping area would be needed to better discriminate the possibility of other activation patterns, such as transient colliding waves. We only mapped the PLAW; therefore, the role played by sources originating outside the PV-LAJ is unknown. However, the importance of non pulmonary veins sources seems limited in paroxysmal AF maintenance (2). We can not completely rule out the possibility that peak adenosine effect coincided with fractionation (15). In addition to the proposed Doppler Effect mechanism, acceleration of fixed sources could also explain our findings, however these should involve external factors which are not likely to account for transitions that occur several times each minute. Finally, no correlation between fractionated electrograms and ganglionated plexi location can be made based on this study.

Supplementary Material

Refer to Web version on PubMed Central for supplementary material.

Acknowledgments

We are grateful to Dr. José Jalife for thoughtful discussions.

Supported in part by grants from the Spanish Society of Cardiology (DC); NHLBI grants P01-HL039707, P01-HL87226, and R01-HL060843 (OB); and the Ministerio Ciencia e Investigación, Red RECAVA (FA, JA, EGT, and FFA) and the Centro Nacional de Investigaciones Cardiovasculares (proyecto CNIC-13) to (FA, JA, EGT, OB).

Abbreviations

AF	atrial fibrillation
CFAE	complex fractionated atrial electrograms (defined in reference 4)
DF	dominant frequency
PLAW	posterior left atrial wall
PV-LAJ	pulmonary vein-lft atrial junctions
SI	systolic interval

REFERENCES

1. Haïssaguerre M, Jaïs P, Shah DC, et al. Spontaneous initiation of atrial fibrillation by ectopic beats originating in the pulmonary veins. N Engl J Med. 1998; 339:659–666. [PubMed: 9725923]
2. Sanders P, Berenfeld O, Hocini M, et al. Spectral analysis identifies sites of high-frequency activity maintaining atrial fibrillation in humans. Circulation. 2005; 112:789–797. [PubMed: 16061740]
3. Oral H, Scharf C, Chugh A, et al. Catheter ablation for paroxysmal atrial fibrillation: segmental pulmonary vein ostial ablation versus left atrial ablation. Circulation. 2003; 108:2355–2360. [PubMed: 14557355]
4. Nademanee K, McKenzie J, Kosar E, et al. A new approach for catheter ablation of atrial fibrillation: mapping of the electrophysiologic substrate. J Am Coll Cardiol. 2004; 43:2044–2053. [PubMed: 15172410]
5. Di Biase L, Elayi CS, Fahmy TS, et al. Atrial Fibrillation Ablation Strategies for Paroxysmal Patients: Randomized Comparison Between Different Techniques. Circ Arrhythmia Electrophysiol. 2009; 2:113–119.
6. Konings KT, Kirchhof CJ, Smeets JR, Wellens HJ, Penn OC, Allessie MA. High-density mapping of electrically induced atrial fibrillation in humans. Circulation. 1994; 89:1665–1680. [PubMed: 8149534]
7. Berenfeld O, Zaitsev AV, Mironov SF, Pertsov AM, Jalife J. Frequency-dependent breakdown of wave propagation into fibrillatory conduction across the pectinate muscle network in the isolated sheep right atrium. Circ Res. 2002; 90:1173–1180. [PubMed: 12065320]
8. Zlochiver S, Yamazaki M, Kalifa J, Berenfeld O. Rotor meandering contributes to irregularity in electrograms during atrial fibrillation. Heart Rhythm. 2008; 5:846–854. [PubMed: 18534369]
9. Rostock T, Rotter M, Sanders P, et al. High-density activation mapping of fractionated electrograms in the atria of patients with paroxysmal atrial fibrillation. Heart Rhythm. 2006; 3:27–34. [PubMed: 16399048]
10. Ortiz J, Niwano S, Abe H, Rudy Y, Johnson NJ, Waldo AL. Mapping the conversion of atrial flutter to atrial fibrillation and atrial fibrillation to atrial flutter. Insights into mechanisms. Circ Res. 1994; 74:882–894. [PubMed: 8156635]

11. Wells JL, Karp RB, Kouchoukos NT, Maclean WAH, James TN, Waldo AL. Characterization of atrial fibrillation in man: Studies following open heart surgery. PACE. 1978; 1:426–438. [PubMed: 95635]
12. Klos M, Calvo D, Yamazaki M, et al. The atrial septopulmonary bundle of the posterior left atrium provides a substrate for AF initiation in a model of pulmonary vein tachycardia of the structurally normal heart. Circ Arrhythmia Electrophysiol. 2008; 1:175–183.
13. Kalifa J, Tanaka K, Zaitsev AV, et al. Mechanisms of wave fractionation at boundaries of high-frequency excitation in the posterior left atrium of the isolated sheep heart during atrial fibrillation. Circulation. 2006; 113:626–633. [PubMed: 16461834]
14. Roberts-Thomson KC, Stevenson IH, Kistler PM, et al. Anatomically determined functional conduction delay in the posterior left atrium. J Am Coll Cardiol. 2008; 51:856–62. [PubMed: 18294572]
15. Atienza F, Almendral J, Moreno J, et al. Activation of inward rectifier potassium channels accelerates atrial fibrillation in humans: evidence for a reentrant mechanism. Circulation. 2006; 114:2434–2442. [PubMed: 17101853]
16. Kneller J, Zou R, Vigmond EJ, Wang Z, Leon LJ, Nattel S. Cholinergic atrial fibrillation in a computer model of a two-dimensional sheet of canine atrial cells with realistic ionic properties. Circ Res. 2002; 90(9):E73–87. [PubMed: 12016272]
17. Davidenko JM, Pertsov AV, Salomonsz R, Baxter W, Jalife J. Stationary and drifting spiral waves of excitation in isolated cardiac muscle. Nature. 1992; 355(6358):349–351. [PubMed: 1731248]
18. Tai CT, Chen SA, Tzeng JW, et al. Prolonged fractionation of paced right atrial electrograms in patients with atrial flutter and fibrillation. J Am Coll Cardiol. 2001; 37:1651–1657. [PubMed: 11345380]
19. Stiles MK, Brooks AG, Kuklik P, et al. High-density mapping of atrial fibrillation in humans: relationship between high-frequency activation and electrogram fractionation. J Cardiovasc Electrophysiol. 2008; 19:1245–1253. [PubMed: 18662185]
20. Ravelli F, Masè M, Del Greco M, Faes L, Disertori M. Deterioration of organization in the first minutes of atrial fibrillation: a beat-to-beat analysis of cycle length and wave similarity. J Cardiovasc Electrophysiol. 2007; 18:60–65. [PubMed: 17229301]
21. Markides V, Schilling RJ, Ho SY, Chow AWC, Davies DW, Peters NS. Characterization of left atrial activation in the intact human heart. Circulation. 2003; 107:733–739. [PubMed: 12578877]
22. Roux J, Gojraty S, Bala R, et al. Effect of pulmonary vein isolation on the distribution of complex fractionated electrograms in humans. Heart Rhythm. 2009; 6:156–160. [PubMed: 19187903]

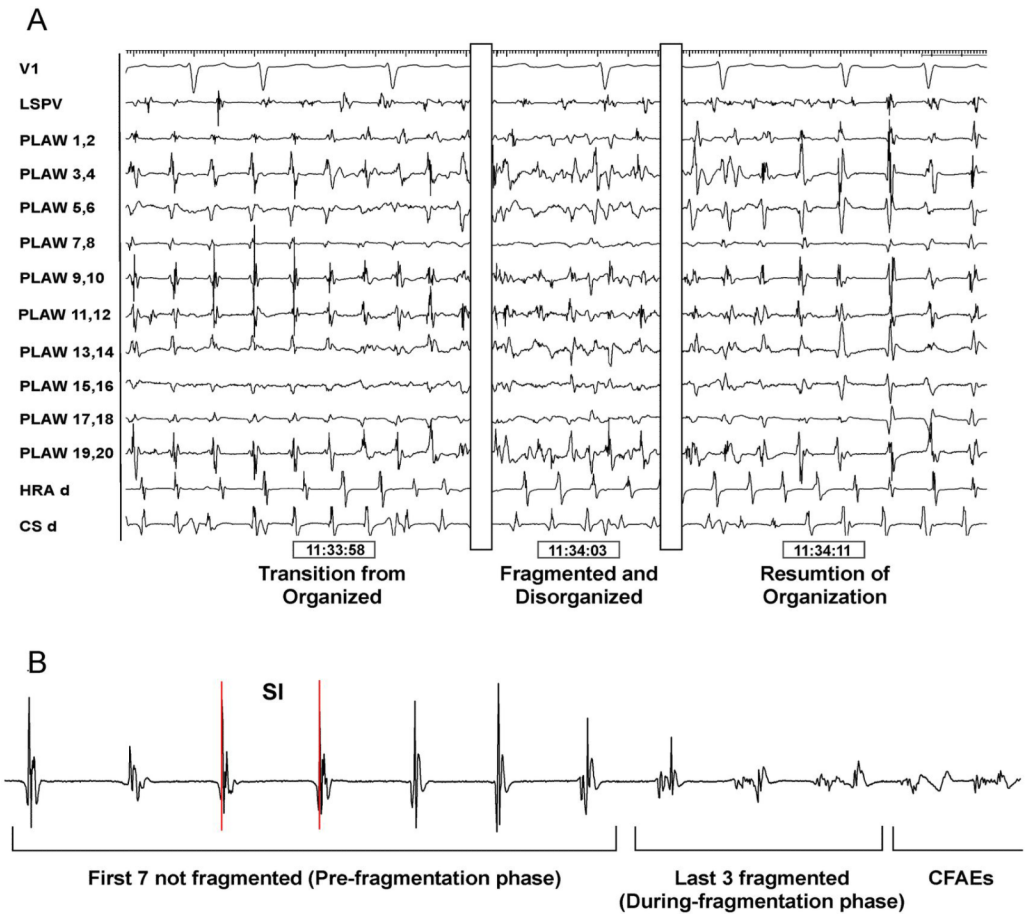

Figure 1. Transitions between organized and fragmented phases

A. Posterior left atrial wall (PLAW) intracardiac recordings using a 20 electrodes spiral catheter. From left o right, transitions from organized to fragmented and back to organized electrograms. **B.** Ten consecutive electrograms were analyzed prior to fragmentation: last 7 organized electrograms (*pre-fragmentation phase*) and first 3 electrograms showing fragmentation (*during-fragmentation phase*). CFAE, complex fractionated atrial electrograms; CS, coronary sinus; HRA, high right atrium; SI, systolic interval.

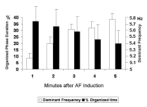

Figure 2. Time courses of organization and dominant frequency

Posterior left atrial wall temporal changes in the percent of organized phases duration (black bars) and dominant frequency (white) after induction.

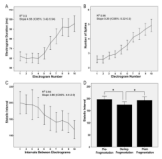

Figure 3. Electrogram characteristics and systolic interval (SI) during transitions from organized to fragmentation (first 10 complexes)

A. Electrogram duration; **B.** Number of spikes. **C.** SI. **D.** Mean values of SI before and during fragmentation and after resumption of organization.

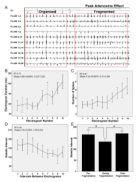

Figure 4. Adenosine infusion

A. Tracings during peak adenosine effect. Lead V1 and intracardiac electrograms recorded from spiral catheter at the posterior left atrial wall (PLAW). At peak adenosine effect (complete AV block) transition from organized to fragmented electrograms is observed, with simultaneous cycle length shortening. **B, C and D.** Electrogram duration, number of spikes and systolic interval (SI) during transitions from organized to fragmented electrograms (first 10 complexes). **E.** Mean values of SI before and during fragmentation, and after resumption of organization.

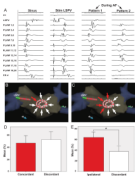

Figure 5. Organized patterns at the posterior left atrial wall

A. Left, activation patterns during sinus rhythm and during stimulation from the left superior pulmonary vein (LSPV). Right, two activation patterns were observed during atrial fibrillation (AF): pattern 1 resembled LSPV stimulation; pattern 2 was similar to sinus rhythm activation. **B and D.** During AF, concordant patterns of activation resembling LSPV stimulation from which AF was induced (red arrow originating at the pacing catheter) accounted for 46±27% of recording time when compared discordant patterns (white arrows). **C and E.** Organized patterns during AF resembling those obtained during pacing from any of the ipsilateral PVs (red arrows originating from the pacing PV side, superior and inferior) accounted for 63±24% of the organized time (p=0.025). CSd, distal coronary sinus.

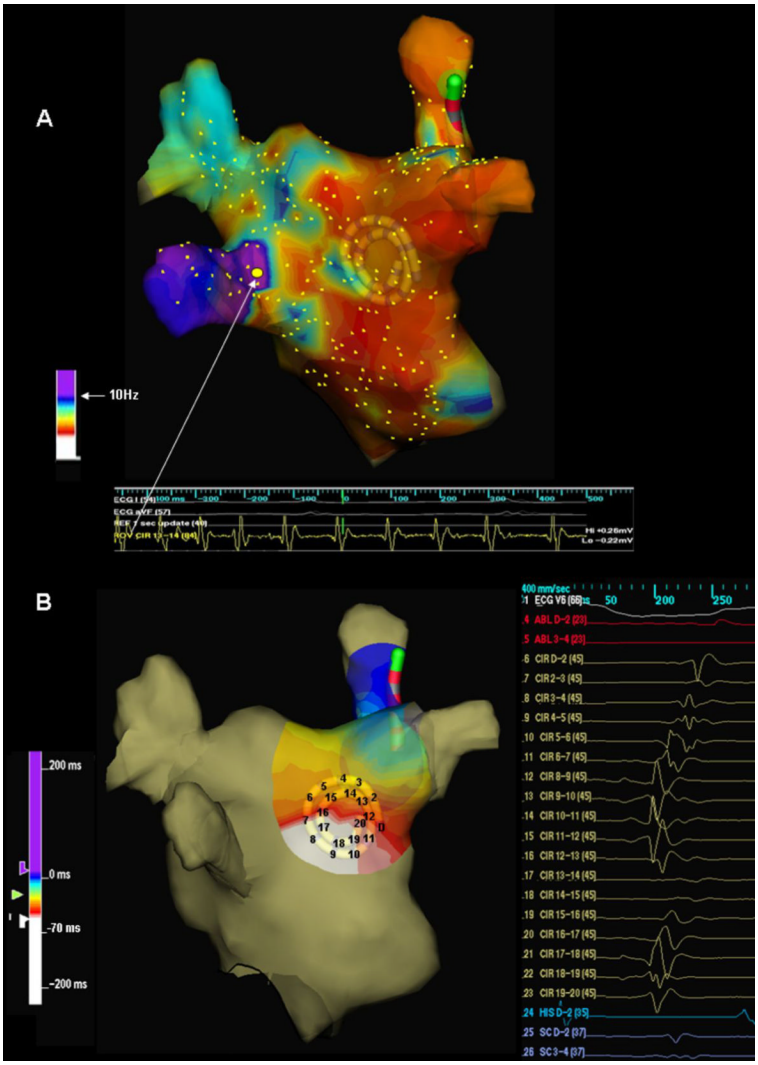

Figure 6. Organized activation patterns in relation to dominant frequency sites location

A. Left atrial dominant frequency (DF) map (posterior view). White arrow points to highest DF site (10.8 Hz) at the left inferior pulmonary vein (LIPV) antrum. **B.** Posterior left atrial wall activation map during organized phase prior to fragmentation (right) shows an incoming wave pattern of activation progressing from closest to the highest DF site at the LIPV (left, white) to the right (purple-blue).

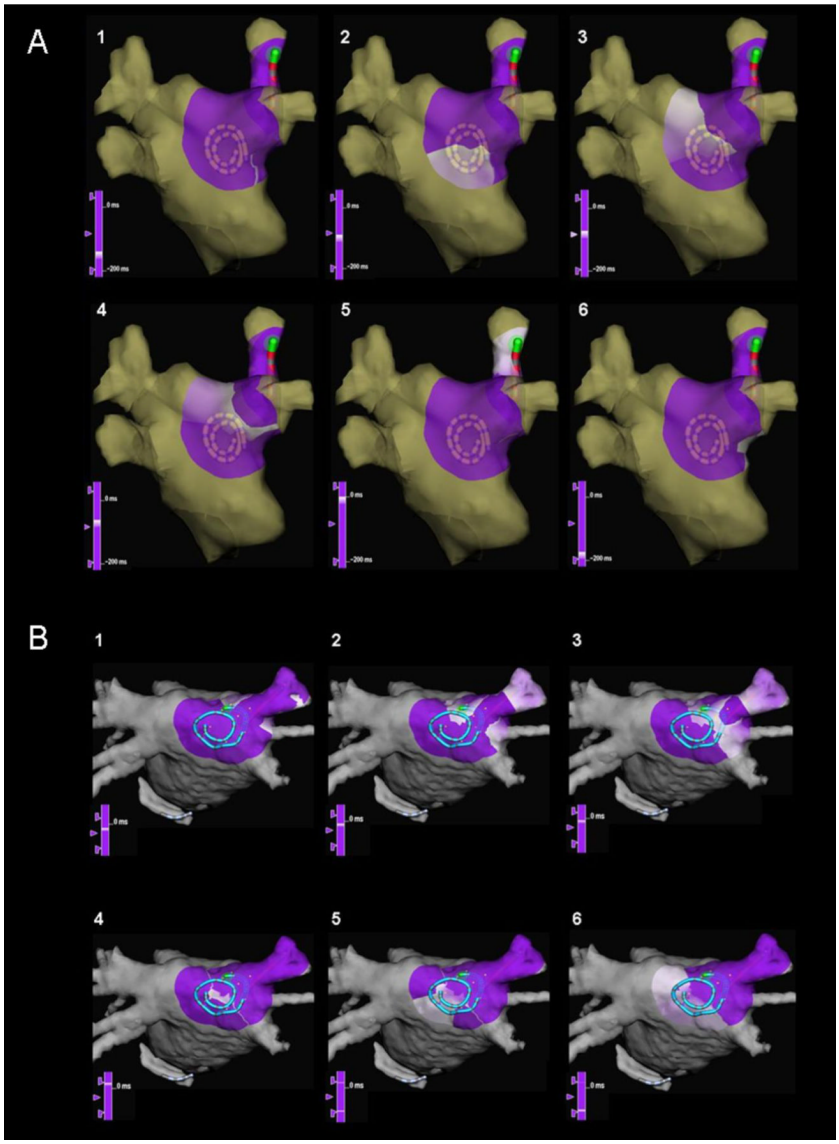

Figure 7. Snapshots of wave propagation at the posterior left atrial wall (PLAW) during transitions to fragmentation

(sequence 1–6): purple, unactivated regions; white, advancing activation. **A.** Reentrant circuit with a clockwise propagation around a pivoting point located to the right edge of the septo-pulmonary bundle. **B.** Activation breakthrough across a line of slow conduction, with activation of the PLAW in both superior and inferior directions, and final convergence on the anterior aspect of the right superior pulmonary vein antrum.

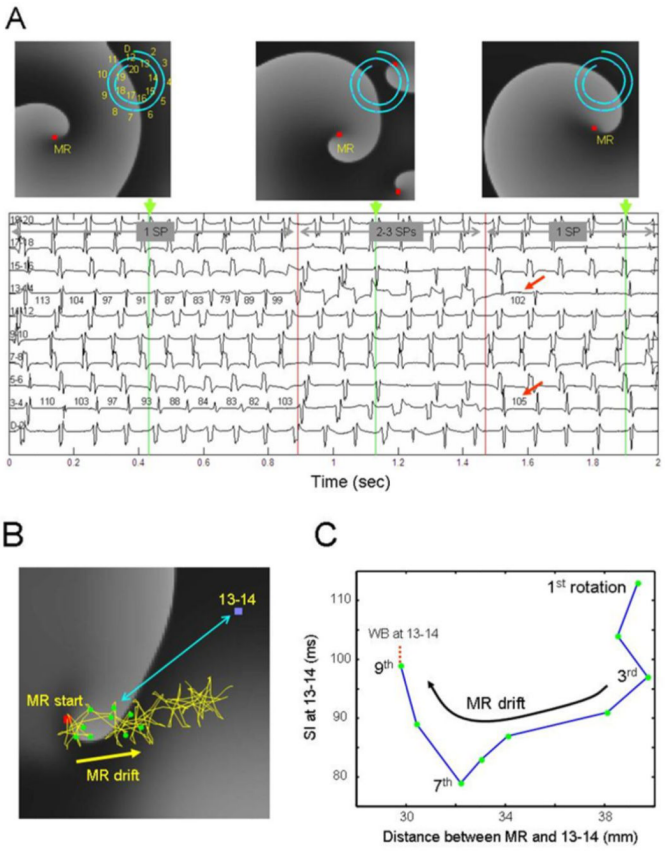

Figure 8. Simulation of a drifting rotor with peripheral wavebreaks (WB) in an atrial model

A. Snapshots of the model membrane voltage are at times indicated by the green markers. A 20 electrode catheter (D-20) shown on snapshots indicates locations of 10 pseudo-bipoles shown below maps. Red squares: Pivoting sites of rotors (i.e., singularity point; SP) Numbers on bipoles 3–4 and 13–14 indicate cycle length in ms. Horizontal gray arrows indicate episodes with a single mother rotor (MR, 1 SP), additional 2 short living rotors after ~0.9 sec (3 SPs) and their disappearance after ~1.5 sec (1 SP). Red arrows denote return of cycle length to pre-shortening phase. **B.** Trajectory of the drifting rotor's tip (yellow trace and arrow) superimposed on a snapshot of voltage at time=0. Red square, starting point of the drift; green dots, the location of the tip at the completion of each of 9 initial rotations; blue square, location of bipoles 13–14; double-headed blue arrow, distance between 13–14 bipoles and a sample position of the rotor's tip. **C,** Systolic Interval (SI) at bipoles 13–14, as a function of distance between the rotor's tip and the bipoles' location. As the drifting rotor gets closer to the bipoles, SI abbreviates due to Doppler shift, particularly after the 3rd rotation. After the 7th rotation, local conduction impairment at 13–14 increases SI with an eventual WB.